

Hydrothermal synthesis, crystal structure, and luminescence of lanthanide(III) coordination polymers with tetrafluorosuccinate and 1,10-phenanthroline

Xia Li^{a,*}, Yan-Bin Zhang^a, Ying-Quan Zou^b

^a Department of Chemistry, Capital Normal University, 105 Xisanhuan North, Beijing 100048, PR China

^b Department of Chemistry, Beijing Normal University, Beijing 100875, PR China

ARTICLE INFO

Article history:

Received 14 June 2008

Received in revised form 9 September 2008

Accepted 15 September 2008

Available online 30 September 2008

Keywords:

Lanthanide coordination polymer

Tetrafluorosuccinate

Hydrothermal synthesis

Crystal structure

Luminescence

ABSTRACT

Three new coordination polymers $[\text{Nd}_2(\text{TFSA})_3(\text{phen})_2]_n$ (**1**) and $\{[\text{Ln}(\text{TFSA})(\text{phen})(\text{H}_2\text{O})_4] \cdot 0.5(\text{TFSA}) \cdot 2(\text{phen}) \cdot \text{H}_2\text{O}\}_n$ ($\text{Ln} = \text{Sm}$, **2** and Dy , **3**; TFSA = tetrafluorosuccinate; phen = 1,10-phenanthroline) were synthesized and characterized using X-ray structure analyses and luminescence spectroscopy. The **1** has a 2-D network structure through TFSA ligands via bridging/chelating-bridging pentadentate and bridging/bridging tetradentate coordination modes. The **2** and **3** have novel 1-D chain structures, in which adjacent Ln(III) ions are linked through the single μ_2 -bridging TFSA ligands as linkages. The emission spectrum in the NIR of **1** corresponds to the ${}^4\text{F}_{3/2} \rightarrow {}^4\text{I}_{9/2, 11/2, 13/2}$ transitions of Nd(III) ion. The emission spectra of **2** and **3** indicate the typical luminescence characteristics of the Sm(III) and Dy(III) ions, respectively.

© 2008 Elsevier B.V. All rights reserved.

1. Introduction

Luminescent lanthanide complexes have attracted attention due to their potential applications in fluorescence materials, electroluminescent devices, bioassays, and luminescent probes [1–5]. Some trivalent lanthanide ions exhibit good emission, such as in the visible region emitting Sm(III), Eu(III), Tb(III), and Dy(III), and in the near-infrared (NIR) emitting Nd(III), Er(III), and Yb(III). Over the past two decades, many studies have focused on lanthanide complexes with carboxylic acid ligands, which have been used to excite lanthanide ions. In particular lanthanide coordination polymers constructed by multicarboxylate ligands show fascinating structure, and the one-, two- and three-dimension polymers consisting of lanthanide and multicarboxylate have been reported [2–17]. In the field of lanthanide carboxylates complexes, the rigid benzene-multicarboxylates [2–11] and the flexible carboxylate ligands are employed [12–17].

In this work, we use a flexible ligand, namely tetrafluorosuccinic acid (H_2TFSA) to construct lanthanide coordination polymers. The H_2TFSA ligand has advantages compared to other ligands: (i) the flexible ligand can adopt various conformations due to the conformational freedom of the carbon skeleton leading to coordination polymers with novel structures; (ii) its steric hindrance is much smaller than benzene-multicarboxylates; (iii) its two carboxylate groups locate on the relative orientation; (iv) it is a fully fluorinated aliphatic ligand. Fluorinated organic ligands can enhance luminescence intensities of complexes, because of the species containing high-energy C–H, N–H, and/or O–H oscillators significantly

quench the metal excited states nonradiatively, leading to decreased luminescence intensities [9]. Furthermore, the complexes of H_2TFSA with metals were relatively less reported [18–21]. In addition, 1,10-phenanthroline (phen) molecule is a good ligand for Ln(III) ions, it is helpful to increase the rigidity and the thermal stability of complexes, and it can also enhance the luminescent properties of lanthanide complexes due to the antenna effect. In the context, we synthesized three new lanthanide coordination polymers, $[\text{Nd}_2(\text{TFSA})_3(\text{phen})_2]_n$ (**1**) and $\{[\text{Ln}(\text{TFSA})(\text{phen})(\text{H}_2\text{O})_4] \cdot 0.5(\text{TFSA}) \cdot 2(\text{phen}) \cdot \text{H}_2\text{O}\}_n$ ($\text{Ln} = \text{Sm}$, **2** and Dy , **3**). Herein, the syntheses, structural characteristics, and luminescence of the three complexes were reported.

2. Experimental

2.1. Synthesis of the complexes

All reagents used for synthesis were of analytical grade and used without further purification, except that the hydrated lanthanide chlorides were prepared by reaction of lanthanide oxides Ln_2O_3 ($\text{Ln} = \text{Nd}$, Sm , and Dy) and hydrochloric acid.

Synthesis of $[\text{Nd}_2(\text{TFSA})_3(\text{phen})_2]_n$ (**1**): a mixture of $\text{NdCl}_3 \cdot \text{H}_2\text{O}$ (0.0717 g, 0.2 mmol), tetrafluorosuccinic acid (0.0570 g, 0.3 mmol), 1,10-phenanthroline (0.0769 g, 0.4 mmol), deionized water (7 ml), and sodium hydroxide aqueous solution (2 mol L^{-1} , 0.40 ml) was placed in a 25 ml Teflon-lined stainless steel autoclave. After stirred, the mixture was sealed and heated at 110 °C for 5 days under autogenous pressure and then slowly cooled to room temperature. After filtration, the product was washed with water, and then

* Corresponding author. Tel./fax: +86 10 68902320.

E-mail address: xiali@mail.cnu.edu.cn (X. Li).

colorless block-like single crystals suitable for X-ray diffraction were obtained in 58% yield (based on Nd). Anal. Calcd (%) for $C_{36}H_{16}F_{12}N_4O_{12}Nd_2$ (1213.00): C, 35.65; H, 1.33; N, 4.79. Found:

Table 1
Crystallographic data and structure refinement for complexes 1–3

Complexes	1	2	3
Empirical formula	$C_{36}H_{16}F_{12}N_4O_{12}Nd_2$	$C_{42}H_{34}F_6N_6O_{11}Sm$	$C_{42}H_{34}F_6N_6O_{11}Dy$
Formula weight	1213.00	1063.11	1075.25
Temperature (K)	294(2)	273(2)	273(2)
Crystal system	Monoclinic	Triclinic	Triclinic
Space group	$C2/c$	$P\bar{1}$	$P\bar{1}$
<i>a</i> (Å)	23.939(3)	7.758(3)	7.747(3)
<i>b</i> (Å)	9.441(11)	14.383(5)	14.343(5)
<i>c</i> (Å)	17.866(2)	20.295(8)	20.210(7)
α (°)	90.00	100.227(2)	100.417(2)
β (°)	101.598(2)	98.622(2)	98.540(2)
γ (°)	90.00	105.514(2)	105.377(2)
<i>V</i> (Å ³)	3955.2(8)	2100.3(14)	2083.4(13)
<i>Z</i>	8	2	2
Dc (mg/m ³)	2.037	1.681	1.714
Absorption coefficient (mm ⁻¹)	2.722	1.494	1.890
<i>F</i> (000)	2336	1064	1072
Crystal size (mm)	0.22 × 0.18 × 0.12	0.38 × 0.26 × 0.20	0.36 × 0.22 × 0.18
θ range for data collection (°)	1.74–26.39	1.04–28.39	1.05–28.30
Limiting indices	$-29 \leq h \leq 29$ $-9 \leq k \leq 11$ $-22 \leq l \leq 22$	$-10 \leq h \leq 10$ $-19 \leq k \leq 19$ $-27 \leq l \leq 27$	$-10 \leq h \leq 10$ $18 \leq k \leq 19$ $-26 \leq l \leq 26$
Reflections collected/unique	10989/4041	30928/10535	29857/10365
Completeness to $\theta = 28.31^\circ$	[$R_{int} = 0.0300$] 99.6%	[$R_{int} = 0.0271$] 96.5 %	[$R_{int} = 0.0308$] 90.1 %
Data/restraints/parameters	4041/54/326	10535/6/635	10365/0/635
Goodness-of-fit on F^2	1.033	1.034	1.044
Final <i>R</i> indices [$I > 2\sigma(I)$]	$R_1 = 0.0204$	$R_1 = 0.0360$	$R_1 = 0.0273$
<i>R</i> indices (all data)	$wR_2 = 0.0443$ $R_1 = 0.0277$ $wR_2 = 0.0467$	$wR_2 = 0.0962$ $R_1 = 0.0415$ $wR_2 = 0.1014$	$wR_2 = 0.0594$ $R_1 = 0.0347$ $wR_2 = 0.0696$
Largest diff. peak and hole (e/Å ³)	0.521 and -0.649	0.877 and -0.699	0.621 and -0.579

Table 2
Selected bond lengths (Å) and angles (°) for complex 1

Nd(1)–O(1)	2.411(19)	Nd(1)–O(4)#1	2.416(18)
Nd(1)–O(3)	2.435(18)	Nd(1)–O(6)	2.444(18)
Nd(1)–O(5)	2.453(18)	Nd(1)–O(2)#2	2.614(19)
Nd(1)–O(1)#2	2.790(19)	Nd(1)–N(1)	2.602(2)
Nd(1)–N(2)	2.627(2)		
O(1)–Nd(1)–O(4)#1	94.70(7)	O(1)–Nd(1)–O(3)	74.09(6)
O(4)#1–Nd(1)–O(3)	71.82(7)	O(1)–Nd(1)–O(6)	73.38(6)
O(4)#1–Nd(1)–O(6)	75.34(6)	O(3)–Nd(1)–O(6)	130.93(7)
O(1)–Nd(1)–O(5)	76.44(6)	O(4)#1–Nd(1)–O(5)	146.59(7)
O(3)–Nd(1)–O(5)	74.77(7)	O(6)–Nd(1)–O(5)	129.89(6)
O(1)–Nd(1)–O(2)#2	118.84(6)	O(4)#1–Nd(1)–O(2)#2	136.69(7)
O(3)–Nd(1)–O(2)#2	140.12(7)	O(6)–Nd(1)–O(2)#2	88.16(7)
O(5)–Nd(1)–O(2)#2	72.70(7)	O(1)–Nd(1)–O(1)#2	71.68(7)
O(4)#1–Nd(1)–O(1)#2	140.05(6)	O(3)–Nd(1)–O(1)#2	134.06(6)
O(6)–Nd(1)–O(1)#2	64.84(6)	O(5)–Nd(1)–O(1)#2	68.15(6)
O(2)#2–Nd(1)–O(1)#2	48.12(5)	O(1)–Nd(1)–N(1)	142.55(7)
O(4)#1–Nd(1)–N(1)	94.72(7)	O(3)–Nd(1)–N(1)	74.67(7)
O(6)–Nd(1)–N(1)	144.00(7)	O(5)–Nd(1)–N(1)	75.85(7)
O(1)–Nd(1)–N(2)	153.86(7)	O(4)#1–Nd(1)–N(2)	72.78(7)
O(3)–Nd(1)–N(2)	120.90(7)	O(6)–Nd(1)–N(2)	81.16(7)
O(5)–Nd(1)–N(2)	126.34(7)	O(2)#2–Nd(1)–N(2)	65.17(6)
N(1)–Nd(1)–O(2)#2	75.52(6)	N(1)–Nd(1)–O(1)#2	119.19(6)
N(2)–Nd(1)–O(1)#2	102.94(6)	N(1)–Nd(1)–N(2)	62.89(8)

Symmetry transformations used to generate equivalent atoms: #1 $-x+2, -y, -z+2$; #2 $-x+2, y, -z+3/2$.

C, 35.61; H, 1.32; N, 4.62. Selected IR (KBr pellet, ν/cm^{-1}): 1658 vs (ν_{asCOO^-}), 1421 s (ν_{sCOO^-}), 1384 s (ν_{phen}), 1232 m (ν_{sCOO^-}), 1128 vs (ν_{phen}), 848 m, 727 s ($\delta_{\text{phen(C-H)}}$), 634 m, 541 m, 412 w ($\nu_{\text{Nd-O}}$).

Synthesis of $\{[\text{Sm}(\text{TFSA})(\text{phen})(\text{H}_2\text{O})_4] \cdot 0.5(\text{TFSA}) \cdot 2(\text{phen})\text{H}_2\text{O}\}_n$ (**2**): The synthetic procedure of **2** was similar to that of **1** except $\text{NdCl}_3 \cdot \text{H}_2\text{O}$ was replaced by $\text{SmCl}_3 \cdot 6\text{H}_2\text{O}$ (0.0729 g, 0.2 mmol) and the amount of sodium hydroxide aqueous solution (2 mol L⁻¹, 0.33 ml). Colorless block-like crystals of **2** were obtained in 43% yield (based on Sm). Anal. Calcd (%) for $C_{42}H_{34}F_6N_6O_{11}\text{Sm}$ (1063.11): C, 47.45; H, 3.22; N, 7.90. Found: C, 47.21; H, 3.45; N, 8.26. Selected IR (KBr pellet, ν/cm^{-1}): 3386 br ($\nu_{\text{O-H}}$), 1677 vs, 1624 s (ν_{asCOO^-}), 1425 m (ν_{sCOO^-}), 1375 m, 1120 vs (ν_{phen}), 844 m, 729 m ($\delta_{\text{phen(C-H)}}$), 636 m, 540 w, 414 w ($\nu_{\text{Sm-O}}$).

Synthesis of $\{[\text{Dy}(\text{TFSA})(\text{phen})(\text{H}_2\text{O})_4] \cdot 0.5(\text{TFSA}) \cdot 2(\text{phen})\text{H}_2\text{O}\}_n$ (**3**): The synthetic procedure of **3** was similar to that of **1** except $\text{NdCl}_3 \cdot \text{H}_2\text{O}$ was replaced by $\text{DyCl}_3 \cdot \text{H}_2\text{O}$ (0.0754 g, 0.2 mmol) and the amount of sodium hydroxide aqueous solution (2 mol L⁻¹, 0.24 ml). Colorless block-like crystals of **3** were obtained in 48.3% yield (based on Dy). Anal. Calcd (%) for $C_{42}H_{34}F_6N_6O_{11}\text{Dy}$ (1075.25): C, 46.92; H, 3.19; N, 7.81. Found: C, 46.65; H, 3.01; N, 7.99. Selected IR (KBr pellet, ν/cm^{-1}): 3386 br ($\nu_{\text{O-H}}$), 1681 vs, 1631 s (ν_{asCOO^-}), 1425 m (ν_{sCOO^-}), 1375 m, 1122 m (ν_{phen}), 852 m, 727 m ($\delta_{\text{phen(C-H)}}$), 632 m, 539 w, 418 w ($\nu_{\text{Dy-O}}$).

Table 3
Selected bond lengths (Å) and angles (°) for complex 2

Sm(1)–O(5)	2.322(3)	Sm(1)–O(2)	2.373(3)
Sm(1)–O(8)#1	2.378(3)	Sm(1)–O(4)	2.411(2)
Sm(1)–O(1)	2.450(3)	Sm(1)–O(3)	2.473(3)
Sm(1)–N(1)	2.600(3)	Sm(1)–N(2)	2.608(3)
O(5)–Sm(1)–O(2)	107.37(12)	O(5)–Sm(1)–O(8)#1	78.05(10)
O(2)–Sm(1)–O(8)#1	145.10(10)	O(5)–Sm(1)–O(4)	81.67(11)
O(2)–Sm(1)–O(4)	73.29(10)	O(8)#1–Sm(1)–O(4)	73.53(10)
O(5)–Sm(1)–O(1)	73.15(10)	O(2)–Sm(1)–O(1)	72.74(10)
O(8)#1–Sm(1)–O(1)	139.01(9)	O(4)–Sm(1)–O(1)	128.60(10)
O(5)–Sm(1)–O(3)	151.75(11)	O(2)–Sm(1)–O(3)	79.20(11)
O(8)#1–Sm(1)–O(3)	81.56(10)	O(4)–Sm(1)–O(3)	73.89(11)
O(1)–Sm(1)–O(3)	133.83(10)	O(5)–Sm(1)–N(1)	85.10(11)
O(2)–Sm(1)–N(1)	140.18(10)	O(8)#1–Sm(1)–N(1)	73.69(10)
O(4)–Sm(1)–N(1)	146.52(10)	O(1)–Sm(1)–N(1)	75.34(10)
O(3)–Sm(1)–N(1)	107.71(11)	O(5)–Sm(1)–N(2)	136.34(10)
O(2)–Sm(1)–N(2)	83.81(10)	O(8)#1–Sm(1)–N(2)	116.65(10)
O(4)–Sm(1)–N(2)	140.83(9)	O(1)–Sm(1)–N(2)	70.34(10)
O(3)–Sm(1)–N(2)	70.83(10)	N(1)–Sm(1)–N(2)	63.25(9)

Symmetry transformations used to generate equivalent atoms: #1 $x-1, y, z$.

Table 4
Selected bond lengths (Å) and angles (°) for complex 3

Dy(1)–O(8)#1	2.284(2)	Dy(1)–O(2)	2.319(2)
Dy(1)–O(5)	2.331(2)	Dy(1)–O(3)	2.356(3)
Dy(1)–O(4)	2.390(3)	Dy(1)–O(1)	2.418(2)
Dy(1)–N(1)	2.547(2)	Dy(1)–N(2)	2.560(2)
O(8)#1–Dy(1)–O(2)	107.86(9)	O(8)#1–Dy(1)–O(5)	78.31(8)
O(2)–Dy(1)–O(5)	144.33(9)	O(8)#1–Dy(1)–O(3)	81.35(9)
O(2)–Dy(1)–O(3)	73.11(10)	O(5)–Dy(1)–O(3)	73.26(9)
O(8)#1–Dy(1)–O(4)	72.72(9)	O(2)–Dy(1)–O(4)	73.26(10)
O(5)–Dy(1)–O(4)	139.29(9)	O(3)–Dy(1)–O(4)	127.99(10)
O(8)#1–Dy(1)–O(1)	151.63(10)	O(2)–Dy(1)–O(1)	79.66(9)
O(5)–Dy(1)–O(1)	80.39(8)	O(3)–Dy(1)–O(1)	74.70(10)
O(4)–Dy(1)–O(1)	134.68(10)	O(8)#1–Dy(1)–N(1)	83.19(8)
O(2)–Dy(1)–N(1)	141.25(9)	O(5)–Dy(1)–N(1)	73.52(8)
O(3)–Dy(1)–N(1)	145.52(9)	O(4)–Dy(1)–N(1)	75.17(9)
O(1)–Dy(1)–N(1)	108.39(9)	O(8)#1–Dy(1)–N(2)	135.79(8)
O(2)–Dy(1)–N(2)	84.25(9)	O(5)–Dy(1)–N(2)	116.41(8)
O(3)–Dy(1)–N(2)	141.76(8)	O(4)–Dy(1)–N(2)	70.60(9)
O(1)–Dy(1)–N(2)	71.14(10)	N(1)–Dy(1)–N(2)	64.30(8)

Symmetry transformations used to generate equivalent atoms: #1 $x+1, y, z$.

2.2. X-ray crystallography

The X-ray single crystal data collections for three complexes were performed on a Bruker SMART CCD diffractometer equipped with a graphite monochromated Mo K α radiation ($\lambda = 0.71073 \text{ \AA}$). Semiempirical absorption corrections were applied. The structures were solved by direct method and refined by full-matrix least-squares method on F^2 using the SHELXTL-97 software package [22,23]. All non-hydrogen atoms in the complexes were refined anisotropically. The hydrogen

atoms were fixed at their ideal positions. Summary of the crystallographic data and details of the structure refinements are listed in Table 1. The selected bond lengths and bond angles of complexes 1, 2, and 3 are listed in Tables 2–4, respectively.

CCDC-668403, 655772, and 655774 for complexes 1, 2, and 3, respectively, contain the supplementary crystallographic data for this paper. These data can be obtained free of charge from CCDC, 12 Union Road, Cambridge, CB2 1EZ, UK; fax: +44(0)1223-336033; email: deposit@ccdc.cam.ac.uk

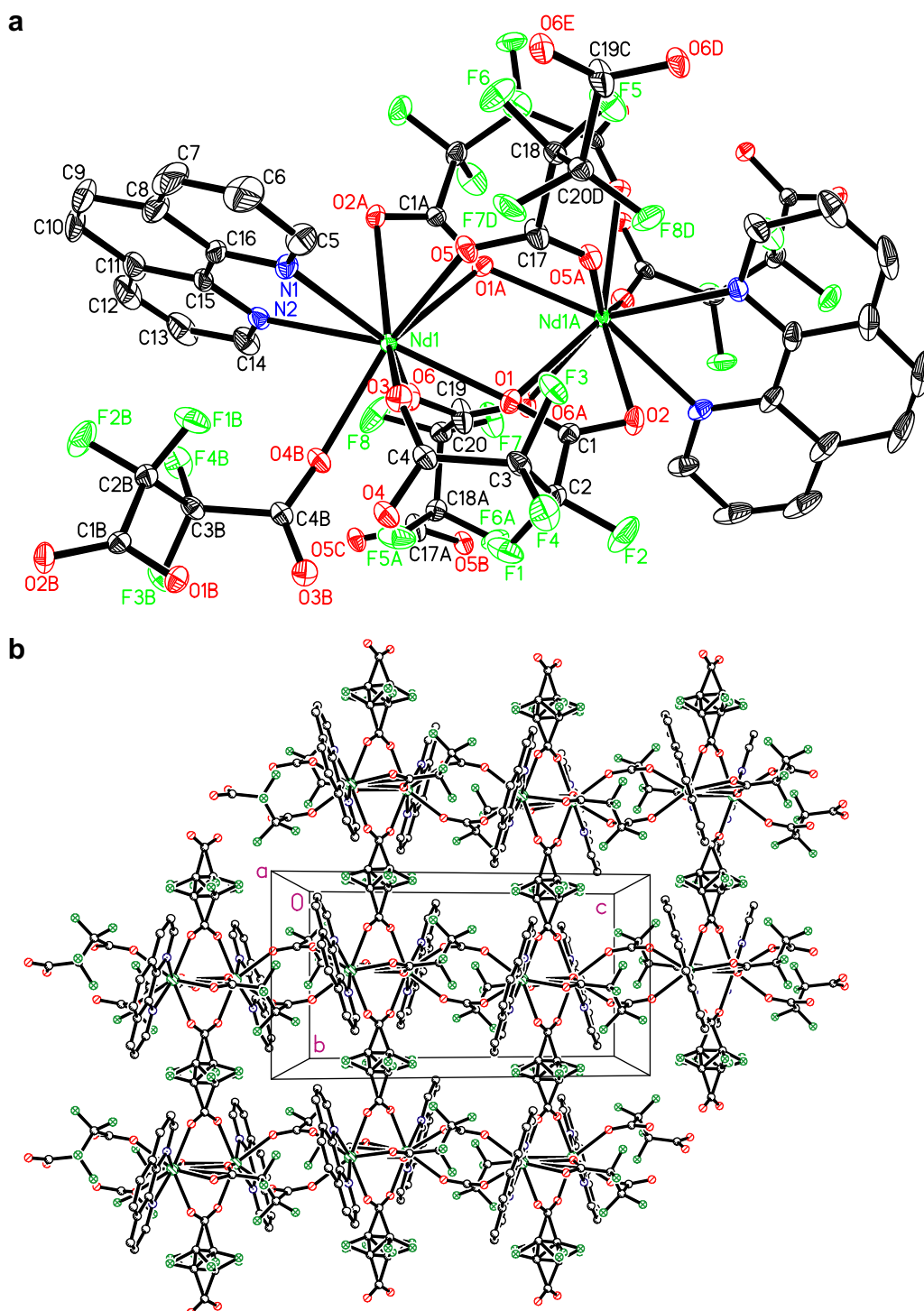


Fig. 1. View of the structure of **1**: (a) coordination geometry of the dimer building block and coordination environment of Nd(III) ion at the 30% probability displacement ellipsoids. (b) 2-D network. All hydrogen atoms are omitted for clarity.

2.3. Physical measurements

Elemental analyses (C, H, N) were performed using an Elementar Vario EL analyzer. IR spectra were recorded with a Bruker EQUINOX-55 spectrometer using the KBr pellet technique. The steady-state near-infrared emission spectra were measured on an Edinburgh FLS920 fluorescence spectrometer equipped with a Hamamatsu R5509-72 supercooled photomultiplier tube at 193 K and a TM300 emission monochromator. Near-IR emission spectra were corrected via a calibration curve supplied with the instrument. Solid-state luminescence spectra were recorded on an F-4500 fluorescence spectrophotometer at room temperature.

3. Results and discussion

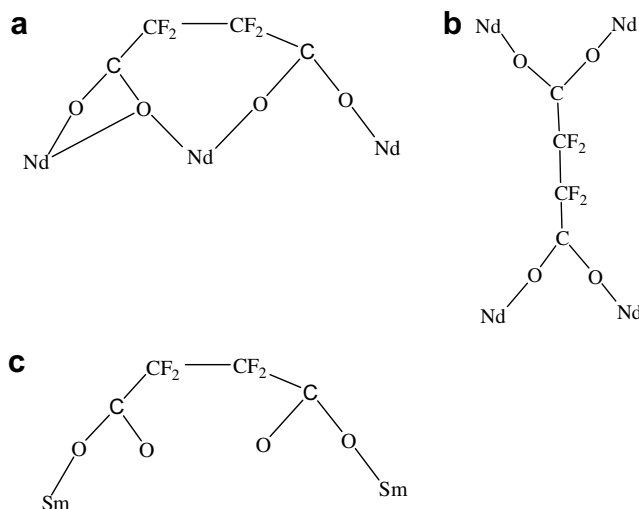
3.1. Structural description of $[Nd_2(TFSA)_3(phen)_2]_n$ (**1**)

The complex **1** consists of a 2-D network, as shown in Fig. 1. The Nd1(III) ion is nine coordinated by seven oxygen atoms of TFSA groups and two nitrogen atoms from phen molecule (Fig. 1a). The Nd1(III) ion is in a distorted monocapped square-antiprism coordination sphere. Atoms O1, O2A, O5, O6 and O3, O4B, N1, N2 form the upper and lower square with mean deviations of 0.1176 and 0.2250 Å, respectively, and the dihedral angle between them is 2.9°. Atom O1A caps the upper plane. The Nd1–O bond lengths vary from 2.411(19) to 2.790(19) Å with the average distance of 2.509 Å. The Nd1–N bond lengths are 2.602(2) and 2.627(2) Å with the average distance of 2.615 Å.

All H_2TFSA ligands deprotonate completely and participate in the coordination to Nd(III) ions in two coordination modes. (i) TFSA ligand coordinates three different Nd(III) ions to form a pentadentate bridge, namely, one carboxylate group of TFSA ligand is in bidentate-bridging mode and another is in bridging-chelating mode (Scheme 1a). (ii) TFSA ligand coordinates four different Nd(III) ions to form a tetradentate bridge, namely, two carboxylate groups of TFSA ligand are in bidentate-bridging mode (Scheme 1b). The two neighboring Nd(III) ions are linked through four COO^- groups of TFSA ligands via bidentate-bridging (e.g., O5–C17–O5A and O6–C19–O6A) and bridging-chelating (e.g., O1–C1–O2 and O1A–C1A–O2A) modes to form a dimeric unit with the distance Nd1(III)–Nd1A(III) ions of 4.220(5) Å. The dimeric units as building blocks are connected to a 1-D chains through pentadentate TFSA ligands along *c*-axis with the distance between two neighboring Nd(III) ions of 6.142(5) Å. These dimeric units are connected to a another 1-D chains through tetradentate TFSA ligands along *b*-axis with the distance between two neighboring Nd(III) ions of 9.441(5) Å. The two types of 1-D chains are further cross-linked to a 2-D network structure (Fig. 1b).

3.2. Structural description of $\{[Ln(TFSA)(phen)(H_2O)_4] \cdot 0.5(TFSA) \cdot 2(phen)H_2O\}_n$ ($Ln = Sm, \mathbf{2}$ and Dy, **3**)

The crystal structure of **2** is given in Fig. 2. The asymmetric unit of **2** consists of $[Sm(TFSA) \cdot phen \cdot (H_2O)_4]$ core (Fig. 2a), free half TFSA ligand, two phen molecules, and a lattice water molecule. The Sm1(III) ion is eight-coordinated by two oxygen atoms from two TFSA ligands, two nitrogen atoms from phen molecule, and the other from four water molecules. The coordination sphere of the Sm(III) ion is a distorted square-antiprism, in which the top square face is defined by O1, O2, O4, and O5, and the bottom one is formed by O3, O8A, N1, and N2. The mean deviations from the upper and lower planes are 0.1693 and 0.088 Å, respectively, and the dihedral angle between the two planes is 6.4°. The Sm1–O(carboxylate) bond distances are 2.322(3) and 2.378(3) Å, respectively, with the average bond distance of 2.35 Å. The Sm1–O(water) bond distances vary in the range of 2.373(3)–2.473(2) Å with the aver-



Scheme 1. The coordination modes of TFSA ligands in **1** and **2**.

age bond distance of 2.472 Å. The Sm1–N bond distances are 2.600(3) and 2.608(3) Å, respectively, with the average bond distance of 2.604 Å.

Adjacent Sm(III) ions are connected through single TFSA ligand to form a 1-D coordination polymer chain (Fig. 2b). Both carboxylate groups of each TFSA ligand coordinate the Sm(III) ion in the rare monodentate fashion (Scheme 1c), and thereby TFSA ligand acts as a μ_2 -bridging ligand. Namely, 1-D chain is formed through the infinite extension $Sm-OOCF_2CF_2COO-Sm$. This is a rare example of lanthanide carboxylate coordination polymers. Many coordination polymers consisting of the assembly of metal centers through multicarboxylate linker show higher dimensional structures, 2-D and 3-D networks [1–9,13–17], 1-D chains are less in lanthanide multicarboxylate complexes [10–12]. However, monodentate coordination mode of carboxylate group and the 1-D chain as **2** formed through single ligand as linker are rare.

In the chain of **2**, TFSA ligand as long bridge links two Sm(III) ions, leading a long Sm(III)–Sm(III) distance of 7.758(3) Å, which is larger than Sm–Sm distances in other reported samarium carboxylate complexes [10,14,17]. Coordinated phen molecules parallel to each other, and the distance of face-to-face is 7.71 Å. Uncoordinated phen molecules are almost parallel with the dihedral angle of 1.1° and the distance of face-to-face between them is 3.24 Å, which indicates π – π stacking interactions of aromatic rings between the uncoordinated phen molecules.

Interestingly, the intermolecular hydrogen bonds are formed between uncoordinated molecules and 1-D coordination polymer chain. Uncoordinated TFSA ligands form hydrogen bonds with coordinated water molecules in the 1-D chain, resulting in a double-chains supramolecular structure (Fig. 2c). Uncoordinated phen molecules are connected to 1-D chain through three kinds of hydrogen bonds, which are formed between coordinated water molecules and uncoordinated phen molecules, O–H...N; uncoordinated water molecules and uncoordinated phen molecules, O–H...N; and uncoordinated water molecules and coordinated water molecules, O–H...O. Distances of the hydrogen bonds are in the range of 2.707(5)–2.919(5) Å (Table 5). Uncoordinated TFSA ligands, phen and water molecules are connected with the 1-D coordination polymer chain through intermolecular hydrogen bonds, which further increases the stability of the structure.

The structural characteristics of **3** are similar to that of **2**. So, the details will not be further discussed in here. The comparison of crystal data between **3** and **2** shows that the average distances of Dy1–O(carboxylate) (2.308 Å), Dy1–O(water) (2.371 Å), Dy1–N

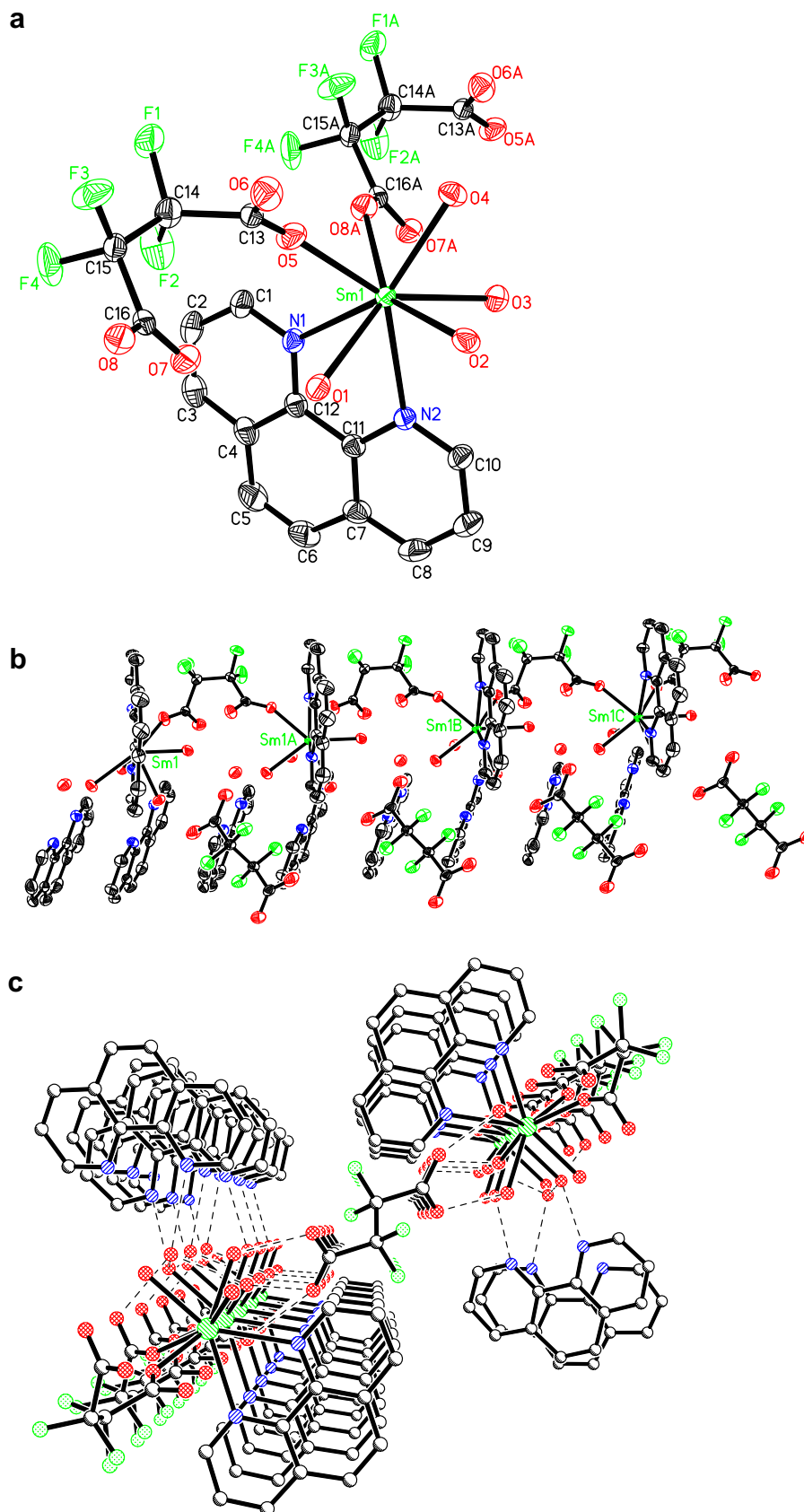


Fig. 2. View of the structure of 2: (a) coordination environment of Sm(III) ion at the 30% probability displacement ellipsoids. The free TFSA, phen, and H₂O are omitted for clarity (b) 1-D chain. (c) Packing diagram viewed along the *a*-axis showing the double-chains structure by hydrogen bonds. All hydrogen atoms are omitted for clarity.

Table 5
Hydrogen bond lengths (Å) and bond angles (°) for complex **2**

D–H...A	d(D...A)	<(DHA)
O(11)–H(11A)...N(5)	2.822(5)	154(6)
O(3)–H(3A)...O(11)	2.707(5)	179(6)
O(1)–H(1B)...O(7)	2.721(4)	158(5)
O(1)–H(1A)...O(9)	2.756(4)	163(5)
O(4)–H(4B)...O(11)	2.717(5)	156(6)
O(4)–H(4A)...N(4)	2.735(4)	168(4)
O(2)–H(2B)...N(3)	2.761(4)	158(5)
O(2)–H(2A)...O(10)	2.680(4)	172(5)
O(11)–H(11B)...O(6)#1	2.803(5)	155(5)
O(3)–H(3B)...O(9)#1	2.919(5)	171(8)

Symmetry transformations used to generate equivalent atoms: #1 $x - 1, y, z$.

(2.553 Å), and Dy1(III)...Dy1A(III) (7.748(3) Å) in **3** are slightly shorter than corresponding distances in **2**, respectively, the reason for that is the radius of the Dy(III) ion is shorter than that of the Sm(III) ion, which is in accordance with the effect of the lanthanide contraction.

3.3. Near-infrared luminescence of the complex **1**

The emission spectrum is presented in Fig. 3. Three infrared emission bands centered around 890, 1061, and 1335 nm, respectively, are assigned to $^4F_{3/2} \rightarrow ^4I_{9/2}$, $^4F_{3/2} \rightarrow ^4I_{11/2}$, and $^4F_{3/2} \rightarrow ^4I_{13/2}$ transitions of Nd(III) ion. Among these emission bands, the $^4F_{3/2} \rightarrow ^4I_{11/2}$ transition is the most intense.

3.4. Visible photoluminescence of complexes **2** and **3**

The solid-state luminescent properties of **2** and **3** were investigated at room temperature. The emission spectrum of **2** was recorded upon excitation wavelength of 345 nm (Fig. 4a). Three emission bands are at 561, 595, and 642 nm, which are attributed to $^4G_{5/2} \rightarrow ^6H_{5/2}$, $^4G_{5/2} \rightarrow ^6H_{7/2}$, and $^4G_{5/2} \rightarrow ^6H_{9/2}$ transitions of Sm(III) ion, respectively. The emission spectrum of **3** upon excitation at 309 nm shows two emission bands at 482 and 571 nm (Fig. 4b), respectively, corresponding to $^4F_{9/2} \rightarrow ^6H_{15/2}$ and $^4F_{9/2} \rightarrow ^6H_{13/2}$ transitions of Dy(III) ion. Further, in the emission spectra of the two complexes, the fluorescent emission of ligands is not observed, indicating an efficient energy transfer from the ligand to the Ln(III) ion. Thus, these observations of emission spectra clearly indicate the typical luminescence characteristics of the Sm(III) and Dy(III) ions caused by the intramolecular energy transfer that consists of the absorption energy by organic ligands, and energy transfer to the Ln(III) ions.

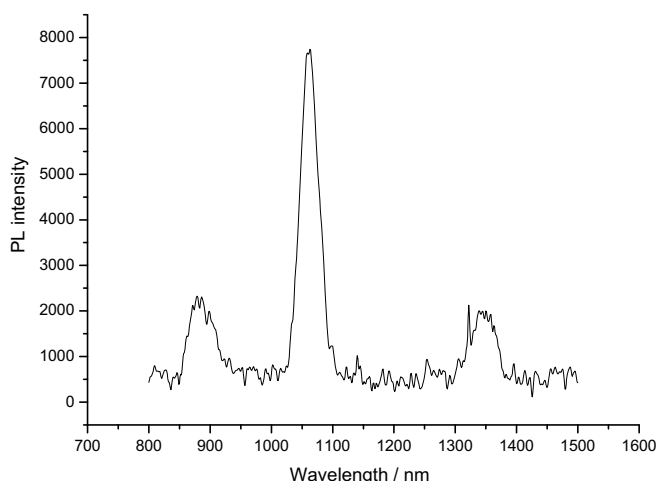


Fig. 3. NIR emission spectrum of **1** at room temperature.

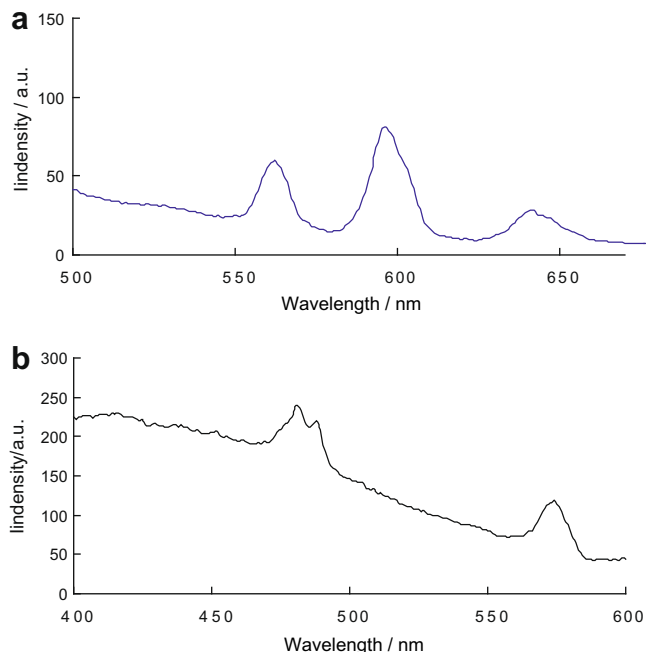


Fig. 4. Emission spectra (a) for **2**, $\lambda_{\text{ex}} = 403$ nm; (b) for **3**, $\lambda_{\text{ex}} = 309$ nm.

4. Conclusions

We have synthesized three lanthanide coordination polymers under hydrothermal condition. The three complexes have two types of crystal structures, in which TFSA ligands adopt the different coordination modes to lanthanide ions. The complex **1** has a 2-D network structure through pentadentate and tetradentate TFSA ligands. The complexes **2** and **3** show novel 1-D structures, in which Ln(III) ions are separated by long and single flexible TFSA anions with its two monodentate carboxylate groups, and relatively long Ln...Ln distances are seen in the **2** and **3**. These structural features are rare in lanthanide carboxylate complexes. The **1** exhibits the near-infrared luminescence of Nd(III) ion. The **2** and **3** exhibit the visible region luminescence of Sm(III) and Dy(III) ions, respectively.

Acknowledgements

We are grateful to the Natural Science Foundation of Beijing (No. 2073022) and the Science and Technology Program, Beijing Municipal Education Commission (KM200510028007).

Appendix A. Supplementary data

Supplementary data associated with this article can be found, in the online version, at doi:10.1016/j.molstruc.2008.09.017.

References

- [1] M.D. Ward, *Coord. Chem. Rev.* 251 (2007) 1663.
- [2] S.K. Ghosh, J.P. Zhang, S. Kitagawa, *Angew. Chem.* 119 (2007) 8111.
- [3] M.L. Cable, J.P. Kirby, K. Sorasaene, H.B. Gray, A. Ponce, *J. Am. Chem. Soc.* 129 (2007) 1474.
- [4] L. Pan, K.M. Adams, H.E. Hernandez, X.T. Wang, C. Zheng, Y. Hattori, K. Kaneko, *J. Am. Chem. Soc.* 125 (2003) 3062.
- [5] T.M. Reineke, M. Eddaoudi, M. Fehr, D. Kelley, O.M. Yaghi, *J. Am. Chem. Soc.* 121 (1999) 1651.
- [6] X.F. Li, Z.B. Han, X.N. Cheng, X.M. Chen, *Inorg. Chem. Commun.* 9 (2006) 1091.
- [7] J.H. Jia, X. Lin, A.J. Blake, N.R. Champness, P. Hubberstey, L. Shao, G. Walker, C. Wilson, M. Schröder, *Inorg. Chem.* 45 (2006) 8838.
- [8] Z.H. Zhang, T. Okamura, Y. Hasegawa, H. Kawaguchi, L.Y. Kong, W.Y. Sun, N. Ueyama, *Inorg. Chem.* 44 (2005) 6219.

- [9] B.L. Chen, Y. Yang, F. Zapata, G.D. Qian, Y.S. Luo, J.H. Zhang, E.B. Lobkovsky, *Inorg. Chem.* 45 (2006) 8882.
- [10] Y.S. Song, B. Yan, *Inorg. Chim. Acta* 358 (2005) 191.
- [11] Y.B. Wang, X.J. Zheng, W.J. Zhuang, L.P. Jin, *Eur. J. Inorg. Chem.* (2003) 3572.
- [12] Z. Rzaczyńska, A. Bartyzel, T. Glowiak, *J. Coord. Chem.* 56 (2003) 1525.
- [13] D.T. de Lill, A. de Bettencourt-Dias, C.L. Cahill, *Inorg. Chem.* 46 (2007) 3960.
- [14] P.I. Girginova, F.A.A. Paz, P.C.R. Soares-Santos, R.A. Sá Ferreira, Luís D. Carlos, V.S. Amaral, Jacek Klinowski, H.I.S. Nogueira, T. Trindade, *Eur. J. Inorg. Chem.* (2007) 4238.
- [15] B. Yu, C.Z. Xie, X.Q. Wang, R.J. Wang, G.Q. Shen, D.Z. Shen, *J. Coord. Chem.* 60 (2007) 1817.
- [16] X. Li, Y.Q. Zou, *J. Coord. Chem.* 59 (2006) 1131.
- [17] X. Li, T.T. Zhang, Z.Y. Zhang, Y.L. Ju, *J. Coord. Chem.* 60 (2007) 2721.
- [18] F.A. Cotton, C.A. Murillo, R.M. Yu, *Inorg. Chim. Acta* 359 (2006) 4811.
- [19] S.Q. Liu, H. Konaka, T.K. Sowa, M. Maekawa, Y. Suenaga, G.L. Ning, M. Munakata, *Inorg. Chim. Acta* 358 (2005) 919.
- [20] M.O. Awaleh, A. Badia, F. Brisse, *Cryst. Growth Design* 5 (2005) 1897.
- [21] Q.M. Wang, G.C. Guo, T.C.W. Mak, *J. Cluster Sci.* 13 (2002) 63.
- [22] G.M. Sheldrick, *Acta Cryst. A* 46 (1990) 467.
- [23] G.M. Sheldrick, Program for X-ray Crystal Structure Solution, University of Göttingen, Germany, 1997.